Plasma Chem Plasma Process (2013) 33:707–723
DOI 10.1007/s11090-013-9454-8

ORIGINAL PAPER

Surface Modification of Smectite Clay Induced by Non-thermal Gliding Arc Plasma at Atmospheric Pressure

Antoine Tiya Djowe · Samuel Laminsi · Daniel Njopwouo · Elie Acayanka · Eric M. Gaigneaux

Received: 20 February 2013 / Accepted: 26 April 2013 / Published online: 9 May 2013

Abstract Smectite clay from Sabga (west-Cameroon) was treated in aqueous suspension by gliding arc plasma to modify its surface properties. The evolution of the modifications was followed with the exposure time and post-discharge duration using Fourier transformed infra red spectroscopy and scanning electron microscopy. X-ray diffraction and nitrogen physisorption analyses were also performed to evaluate if both crystalline and textural properties of the material are affected by the treatment. The results obtained show that the plasma treatment causes the breakdown of structural bounds at the clay surface and induces the formation of new hydroxyl groups (Si–OH and Al–OH) on the clay edges. Crystallinity, sheet structure and textural properties are not significantly affected by the plasma treatment. However, it should be noted that an intensive treatment of the clay lowers the pH of the suspension, which subsequently induces an acid attack of the clay. In such case, the specific surface area of the clay increases. This study demonstrates that gliding arc plasma treatments can be used to activate clay minerals for environmental application.

Keywords Smectite clay · Gliding arc plasma · Humid air · Hydroxyl groups

Introduction

Clay minerals are hydrated aluminosilicates structurally constituted by an arrangement of tetrahedral and octahedral sheets. Montmorillonite and other similar smectite clays consist

A. T. Djowe (✉) · S. Laminsi · D. Njopwouo · E. Acayanka
Inorganic Chemistry Department, University of Yaoundé I, P.O. Box 812, Yaoundé, Cameroon
e-mail: antoine.tiyadjowe@uclouvain.be

A. T. Djowe · E. M. Gaigneaux (✉)
Institute of Condensed Matter and Nanosciences (IMCN), Division "MOlecules, Solids and reactiviTy" (MOST), Université catholique de Louvain, Croix du Sud 2/L7.05.17, 1348 Louvain-la-Neuve, Belgium
e-mail: eric.gaigneaux@uclouvain.be

of one octahedral sheet (O) sandwiched by two tetrahedral sheets (T). They are formed by the agglomeration of TOT layers.

The physicochemical properties of clay minerals and their abundance associated with their relatively low cost justify their numerous traditional uses in ceramics, paper, paint, plastics, drilling fluids, chemical carriers, liquid barriers, discoloration, and in other more advanced applications such as in catalysis [1, 2]. Improvement of mining and processing techniques will lead to further growth of these applications and development of innovative products involving clay minerals [3]. Therefore, natural clays are often the subject, before their uses, of several treatments depending on the intended application. These treatments are thermal, mechanical, acid attack, "pillaring" by inorganic cations, functionalization by organic molecules etc. [4–7]. In this sense, the present paper introduces a new method to treat a cameroonian smectite clay, namely submitting the later to gliding arc plasma (glidarc) in humid air. Our objective is to evaluate the ability of glidarc to modify clays superficial properties. The plasma technique used in this work has the advantage to be environmentally friendly since the reactive species are created without using any additional reagents.

Humid air plasmas are known for their high reactivity due to the plume, which is rich in excited and very reactive radicals ($HO^{\cdot}$, $NO^{\cdot}$, etc.) formed in the electric discharge [8–10]. The interactions between these species and aqueous media account for the formation of active species that cause acidifying and oxidizing effects in the aqueous suspension. The hydroxyl radical $HO^{\cdot}$ is probably the most important species spectroscopically identified [11, 12] in the discharges because of its oxidizing properties. Generally, this species reacts on the substrates in aqueous medium by following a radical mechanism [13, 14]. The acidifying effect of humid air plasma is related to the formation of transient nitrous acid (ONOH) which disproportionates into stable peroxonitrous acid (ONOOH) and its isomer nitric acid (HNO_3) for pH < 6 [15]. The proposed mechanism for the formation of nitrous acid was described as follow [16]:

$$NO + O_2 \rightarrow ONOO$$
$$ONOO + NO \rightarrow ONOONO$$
$$ONOONO \rightarrow 2NO_2$$
$$NO_2 + NO \rightarrow N_2O_3$$
$$N_2O_3 + H_2O \rightarrow 2ONOH$$

This innovative technique was successfully used for oxidizing many compounds such as iron (II) complexes [17], azoïc dyes in textile effluents [18] and spent solvents [19].

The first objective of this study is to investigate whether the reactive species created in plasma medium are able to break down the Si–O–Si and Al–O–Al bounds of the smectite clay edges to form Si–OH functions called "silanol groups" and new Al–OH functions ("aluminol groups"). In fact, smectite clays are largely used to remove cationic dyes and surfactants from aqueous media via adsorption processes because of their high cationic exchange capacity [20, 21]. However, their adsorption capacity toward anionic species remains very low because of the low number of hydroxyl groups present on their surface (only aluminol groups). Our hypothesis is that the plasma treated material with new surface hydroxyls could then be used as low-cost adsorbent to remove anionic species from water/wastewater. The second objective of this work is to evaluate to what extent the expected surface modifications of smectite clay by gliding arc plasma are accompanied by some degradations of the bulk properties of the material, mainly in term of crystallinity, sheet structure and texture.

The surface modifications occurring during plasma treatment are evaluated with respect of the plasma exposure time using Fourier transformed infra red (FTIR) spectroscopy and scanning electron microscopy. The occurrence of temporal post-discharge chemical reactions (TPDR) which are of major interest for industrial application is also evaluated. X-ray diffraction (XRD) analysis and N_2 physisorption are respectively used to evaluate the possible modifications of crystalline and textural properties of the material during treatment.

Materials and Methods

Clay Material

The material used in this study is a natural clay collected in a rich deposit in the west of Cameroon, named Sabga. This clay consists of calcium montmorillonite (*d space* = 14.86 nm) with minor impurities (quartz and feldspar) as ascertained by XRD (Fig. 1).

The bulk chemical composition of this deposit was determined in a previous work by Djoufac et al. [22] and is presented in Table 1.

Instrumentation for the Plasma Discharge

The design of the reactor is the gliding arc reactor as described by Lesueur et al. [23] and by Czernichowski [24] for the decontamination of gases. The equipment consists of a generator (an Aupem Sefli HV transformer: 9 kV; 100 mA in open conditions) operating at high voltage, which produces an arc between two divergent electrodes. This arc is pushed along the diverging electrodes by a gas flow (hereafter named feeding gas) provided by a compressor and directed along the axis of the electrodes. The arc moves along the electrodes to their tips where it bursts into a plasma plume until it is short-circuited and

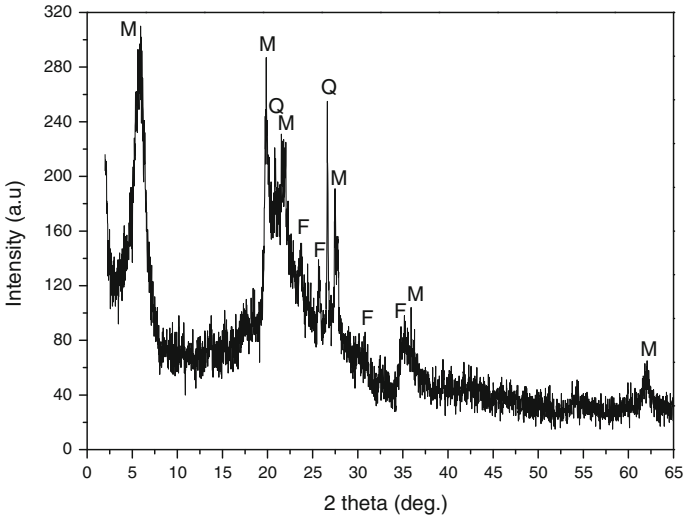

Fig. 1 XRD pattern of raw clay (*M* Montmorillonite, *Q* Quartz, *F* Feldspar)

Table 1 Chemical composition of the clay sample (adapted from [22])

Component	Content (wt%)
SiO_2	63.36
Al_2O_3	14.58
Fe_2O_3	4.24
MnO	<0.03
MgO	0.23
CaO	0.7
Na_2O	0.39
K_2O	2.34
TiO_2	0.2
P_2O_5	<0.05
L.I.[a]	13.79
Total	99.83

[a] L.I.: Loss at ignition (25–1,000 °C)

replaced by a new arc. The length of the arc (which is actually a thermal plasma) gradually increases, and its temperature falls until it breaks and becomes a quenched plasma close to ambient temperature at atmospheric pressure. Such plasma has properties and composition that look like a thermal plasma. In particular, its ionization ratio is likely higher than for corona or DBD discharges, although the energy displayed in the discharge remains less than about 15 eV. The plasma plume is directed to be in contact with the aqueous suspension of clay, so that the active species formed in the discharge are able to react at the liquid surface and with clay particles. The chemical batch reactor in which the treatment was carried out is cooled down and the temperature is maintained between 323 and 333 K to limit evaporation and vapour stripping. Additionally, a magnetic stirring of the suspension was applied. A sketch of the setup is presented in Fig. 2.

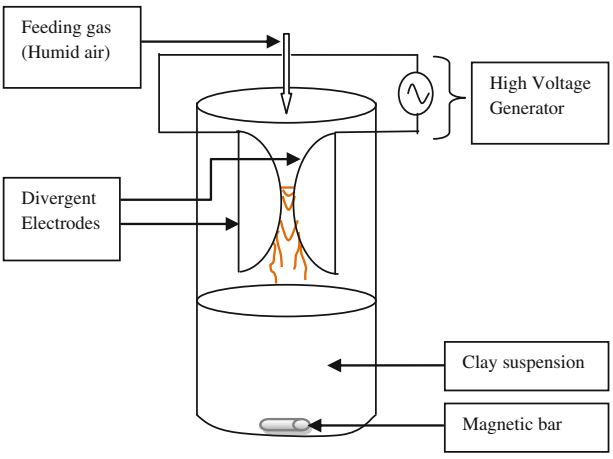

Fig. 2 Scheme of experimental setup

Treatment Procedure

Treatment was carried out using a batch reactor conditions. 10 g of clay with particles size smaller than 63 μm were added to 400 mL of deionised water at a distance of about 50 mm from the electrode tips (Fig. 2). The selected feeding gas was water saturated air provided by a compressor and passing through a bubbling flask of water maintained at 303 K. The feeding gas was provided in the reactor with a flow rate optimized at 800 L h^{-1} and was blown through a nozzle directly into the zone formed between the electrodes. The clay suspension was exposed to the plasma discharge for different times (30, 60, and 120 min). Each aliquot was named Sa*t-00* where *t* (in minutes) represents the exposure time. After the time *t*, the discharge was switched off and the clay suspension was immediately washed with deionized water and dried at 378 K for 1 day. The raw sample was magnetically stirred in aqueous suspension at 333 K for 30 min and dried in the same conditions. This sample was named Sa00-00 and considered as untreated. Another reference sample will be the raw used as such. In order to check the occurrence of temporal post-discharge reactions (TPDR), some samples were left in the suspension after the discharge was switched off. To benefit of such TPDR, the suspension was kept under magnetic stirring for various times after the discharge was switched off. Each aliquot was named Sa*t-d* where *d* (in hours) represents the duration of post-discharge treatment.

Characterisation

Fourier transformed infra red spectra were recorded using an Equinox IFS55 spectrometer (Brücker) equipped with a DTGS detector. The absorption spectra were obtained by recording 100 scans between 400 and 4,400 cm^{-1} with a resolution of 4 cm^{-1}. The powders were diluted in analytical grade KBr (2 mg of clay for 200 mg of KBr) and then pressed into self-supporting disks (13 mm in diameter) before analysis.

Scanning electron microscopy (SEM) analyses were performed with a LEO 983 GEMINI microscope equipped with a field emission gun. The non-metal coated samples were exposed to electrons with an acceleration voltage of 1 kV.

X-ray diffraction analyses were performed on a Siemens D5000 diffractometer using the Kα radiation of Cu ($\lambda = 1.5418$ Å). These analyses were done on the fine fraction of material obtained by siphonation method following the Stocke's law. The diffraction patterns were recorded at a rate of 0.2° min^{-1}, with the machine operated at 40 kV and 40 mA.

Textural analyses were carried out on a Micromeritics Tristar 3000 equipment using N_2 adsorption/desorption at 77 K. Before the measurements, all the samples were outgassed at 423 K overnight under vacuum. BET equation was used to determine surface area.

Results and Discussion

FTIR Spectroscopy

Assignment of IR Bands of Raw Material

Figure 3 shows the FTIR spectrum of the untreated raw material. The assignment of the main bands was done according to Madejóva et al. [25] and Madejóva and Komadel [26].

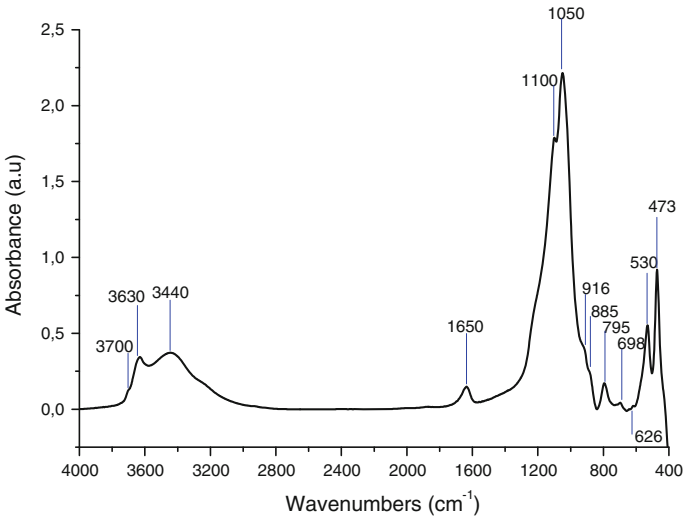

Fig. 3 FTIR spectrum of raw smectite clay

The bands at 3,630 cm^{-1} and the shoulder 3,700 cm^{-1} correspond to stretching vibrations of structural hydroxyls. Those at 3,440 and 1,650 cm^{-1} are assigned to stretching vibrations and deformation of adsorbed water respectively. The most intense band around 1,050 cm^{-1} is attributed to stretching vibrations of Si–O bonds in the tetrahedral layer, while those at 530 and 473 cm^{-1} are due to the deformation of Si–O–Al (where Al is the octahedral cation) and Si–O–Si group respectively. The shoulder at 626 cm^{-1} is related to perpendicular vibrations of octahedral cations (RO–Si) where R=Al, Fe or Mg. The two closely spaced peaks that appear in the deformation region of structural hydroxyl at 916 cm^{-1} (AlAlOH) and 885 cm^{-1} (AlFeOH) are due to isomorphic substitution of aluminium by iron in the octahedral sheets. The quasi absence of a third peak at 850 cm^{-1} indicates the low presence of magnesium in the octahedral sheets. The peaks at 1,100, 795 and 698 cm^{-1} due to the vibration of silica Si–O bonds in quartz indicate that the later is the major impurity in our samples. In the following, this quartz fraction in our samples is used as internal standard for further advanced characterization of our treated clay samples.

Effect of Exposure Time on IR Spectrum of the Clay

Fourier transformed infra red spectra of untreated and plasma treated clay are presented on Fig. 4. These spectra show that exposure of clay material to the plasma discharge induces functional changes in hydroxyls stretching region (Fig. 4a). Indeed, after 30 min of exposure, a new absorption band appears around 3,750 cm^{-1} and increases in intensity with exposure time. In addition, a "zoom" around the peak at 3,630 cm^{-1} indicates the presence of other new bands at 3,650 and 3,668 cm^{-1} on the spectrum of the treated samples.

These modifications are less visible in the framework region (Fig. 4b) showing that the structure of the material is not strongly affected by plasma treatment. However, a decrease in band intensity of the bending vibrations of Si–O–Al (530 cm^{-1}) and Si–O–Si

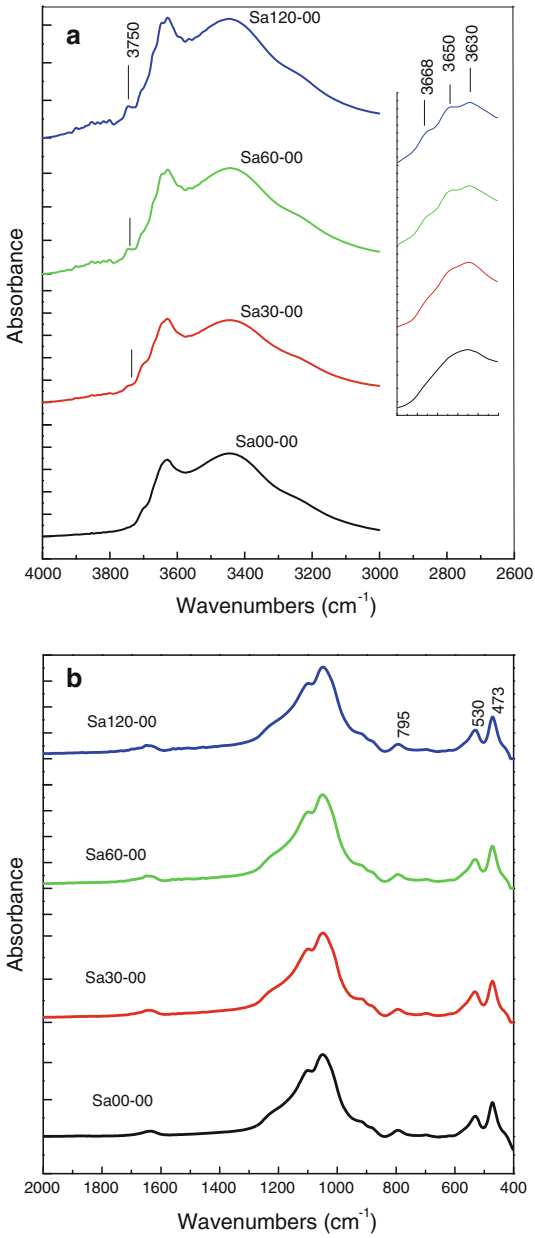

Fig. 4 FTIR spectra of untreated and treated smectites. **a** Hydroxyl region, **b** framework region

(473 cm^{-1}) groups is observed as represented on Fig. 5. The same result can be also obtained for the stretching vibration band of Si–O–Si group at 1,050 cm^{-1}. This result shows that plasma treatment induced the breaking of some structural bonds of clay as a consequence of the radical attack of clay by the $HO^{\cdot}$ radicals or by hydrated electrons present in the aqueous suspension. The same observation was made by Ming and Spark after the treatment of kaolinite by radio frequency plasma [27].

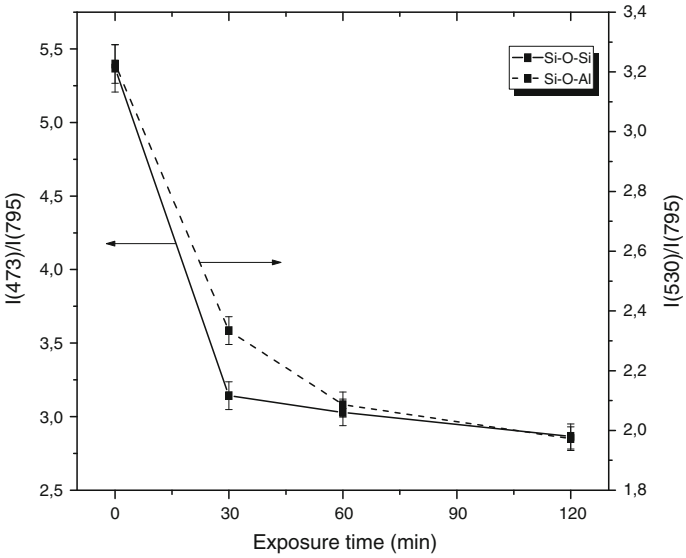

Fig. 5 Evolution of the relative intensities of Si–O–Si and Si–O–Al IR bands as a function of exposure time. The peak at 795 cm^{-1}, previously assigned to the quartz impurity in our samples, is used as internal standard, quartz being considered as totally inert in front of the plasma treatment

Effect of Temporal Post-Discharge Chemical Reactions on IR Spectrum of the Clay

It has already been stated on several examples that substrates exposed to plasma continued to evolve after stopping the discharge [28, 29]. This phenomenon called temporal post-discharge reactions (TPDR) was followed on clay samples treated for 30 and 120 min. Figures 6 and 7 show the evolution of IR spectra of Sa30-d and Sa120-d as a function of the post-discharge time (d). It turns out for Sa30-d that the hydroxylation process continues even after the discharge was switched off since the intensities of the bands at 3,750, 3,668 and 3,630 cm^{-1} increase with the duration of the post-discharge treatment. However, this process is less marked on Sa120-d than on Sa30-d. Moreover, the decrease of Si–O–Si and Si–O–Al band intensities at 473 and 530 cm^{-1} respectively is observed up to 24 h of post-discharge for Sa30-d (Fig. 8a). In the case of Sa120-d, the intensities of these bands decrease slightly but regularly even after 48 h of post-discharge (Fig. 8b). This is due to the contribution of an acid attack of the clay. Indeed, during plasma treatment, the pH of the suspension decreases from 7 to 4 and to 2.5 after 30 and 120 min of treatment respectively. This decrease of pH is the consequence of nitrous and nitric acid formation in the aqueous suspension during plasma treatment. The low pH value of the clay suspension treated for 120 min seems to be sufficient to induce some acid dissolution of the clay particles which is often accompanied by the dehydroxylation of the sheets. This acidification of the medium therefore explains the difference in hydroxylation process between Sa30-d and Sa120-d.

Assignment of FTIR Vibration Bands of Plasma Treated Clay

In order to assign the IR vibration bands of hydroxyls formed on the material after plasma treatment, the spectrum of the reference untreated clay was overlaid on that of Sa30-48

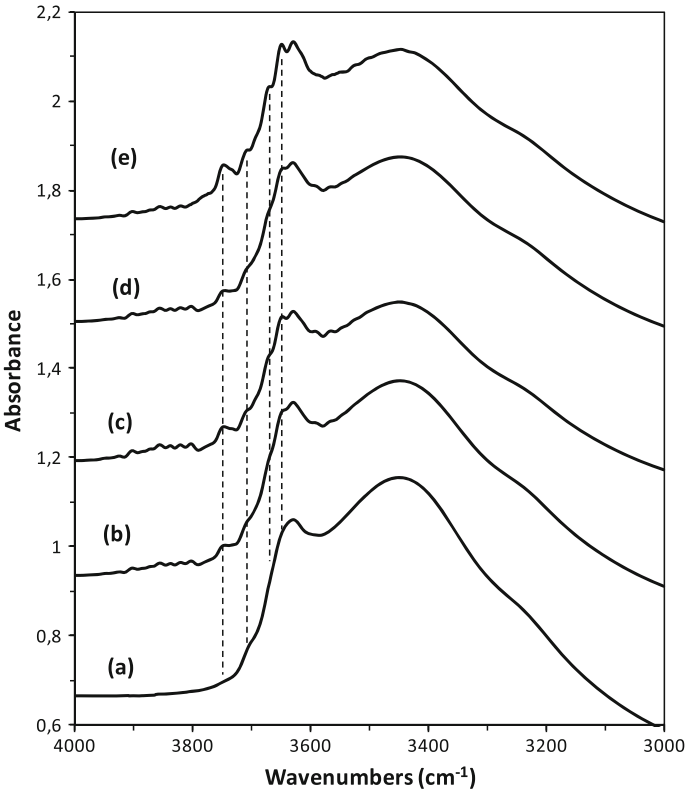

Fig. 6 Influence of TPDR on the IR spectrum of clay treated for 30 min: (*a*) Sa30-00, (*b*) Sa30-06, (*c*) Sa30-12, (*d*) Sa30-24, (*e*) Sa30-48

(Fig. 9). The assignments were done according to Dugas and Chevallier [30] and Khraisheh et al. [31]. The new hydroxyls bands are mainly assigned to the silanol groups (Si–OH). It is however noted that the band intensities of the aluminols vibrations (Al–OH) have remarkably increased during plasma treatment. This result shows that the plasma treatment causes the breakdown of structural bounds at the clay surface and induces the formation of new hydroxyl groups (Si–OH and Al–OH) on the clay edges as summarised on the scheme of Fig. 10. The assignments of the new hydroxyls functions formed on the clay edge after treatment by gliding arc plasma are depicted in Table 2.

Scanning Electron Microscopy (SEM)

The influence of plasma treatment on clay particles morphology is evidenced by SEM micrographs (Fig. 11). Sa00-00 revealed morphology consisting of small aggregates of clay particles. However, it was difficult to determine their exact texture because of particles coalescence. White spots can be observed on SEM images of plasma treated samples. These spots are more numerous for Sa30-48 (Fig. 11c) than for other samples and can be attributed to the changes in morphology due to the hydroxylation process [32].

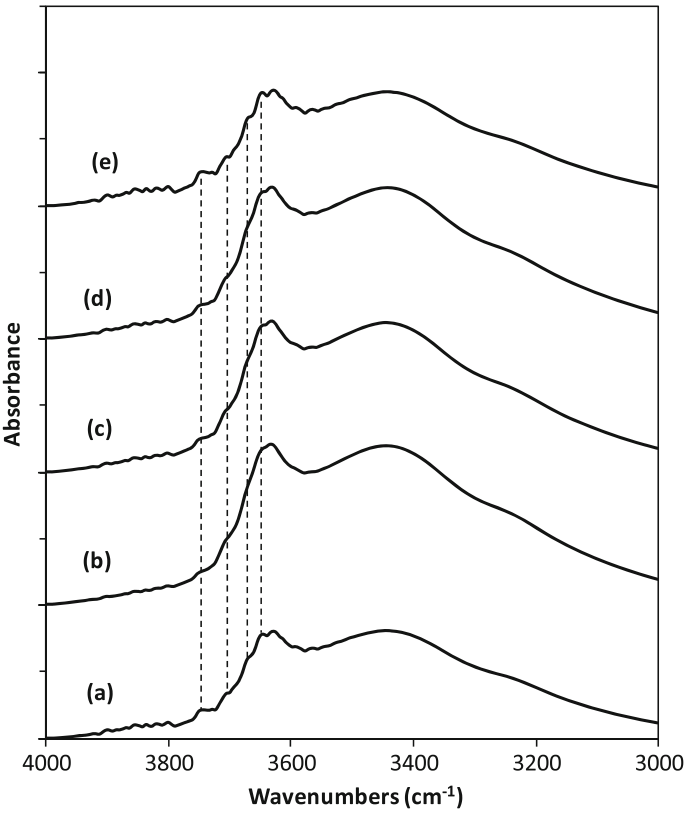

Fig. 7 Influence of TPDR on the IR spectrum of clay treated for 120 min: (*a*) Sa120-00, (*b*) Sa120-06, (*c*) Sa120-12, (*d*) Sa120-24, (*e*) Sa120-48

X-ray Diffraction (XRD)

X-ray diffraction analysis showed few changes in the crystalline structure of clay after plasma treatment (Fig. 12). In fact, the d_{001} reflection of smectite at 14.86 Å decreases in intensity and becomes broader with exposure time. Gliding arc plasma contains $HO^{\cdot}$ radicals and their dimeric form H_2O_2, and these can change the oxidation state of iron ion in clay structure [29]. Thus, the observed variation in the XRD patterns may be due to partial oxidation of octahedral iron that induces a release of some interlayer cations in the aqueous medium. At the end, our samples present a mix of spots where such event occurred inducing a smaller *d* value, and of spots where the oxidation would not have occurred, with *d* remaining at its initial higher value. The co-existence of different spots with two different *d* values corresponds to a certain disorder within our treated samples, which is fully consistent with the observed intensity decrease and the broadening of the parent diffraction peaks. Douglas and Fiessinger actually have similarly reported that during the pre-treatment of clay mineral with hydrogen peroxide to remove organic matter, the intensity of their (001) diffraction line also decreases as a consequence of the partial degradation of the material [33]. At the opposite, further changes in XRD patterns of the clay having been submitted to a post-discharge treatment were not observed (not shown).

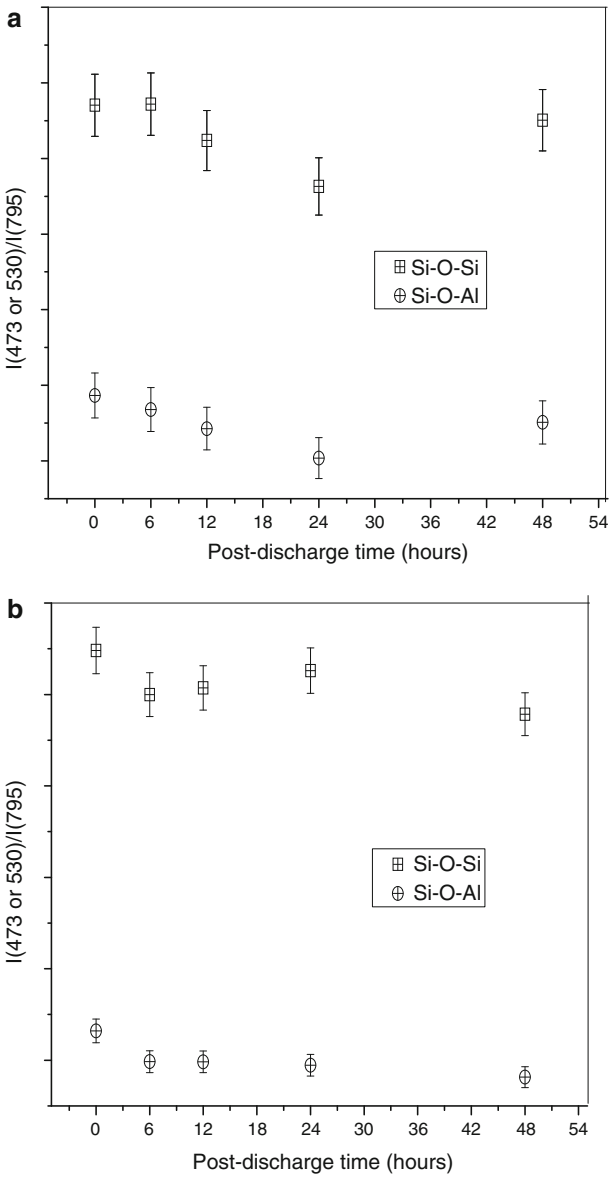

Fig. 8 Evolution of relative intensity of Si–O–Si (473 cm^{-1}) and Si–O–Al (530 cm^{-1}) bands in post-discharge (**a** Sa30-d, **b** Sa120-d). The same use of quartz (as explained in the legend of Fig. 5) as internal standard is made

Nitrogen Physisorption

Figure 13 shows the adsorption–desorption isotherms of untreated and plasma treated clays. For all samples, a type IV isotherm is observed which is typical of mesoporous materials according to IUPAC recommendations [34]. Furthermore, these isotherms contain pronounced type H3 hysteresis loops. Such hysteresis above $P/P_0 = 0.4$ is usually

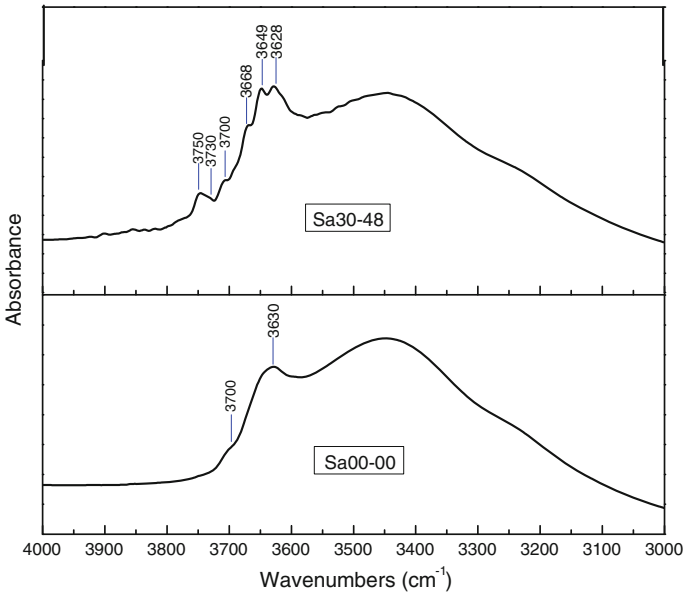

Fig. 9 IR spectra of hydroxyls vibration bands on untreated (Sa00-00) and plasma treated (Sa30-48) clay surface

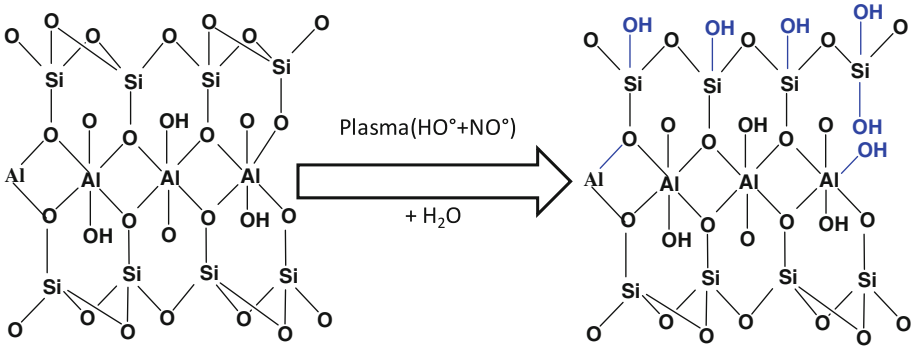

Fig. 10 Scheme showing the formation of the new hydroxyl groups on the clay

attributed to a multilayer formation (adsorption branch) and a capillary decondensation (desorption branch) of N_2 in clays in-between-sheets lamellar mesopores [35–37]. The adsorption–desorption isotherms of the plasma treated samples have the similar shape as the untreated one indicating that the interlayer space of clay particles is not strongly modified during the treatments. Furthermore, the BET surface area remains constant after the plasma treatment (Table 3). However, an increase in surface area from 39 to 45 $m^2\ g^{-1}$ is observed in the post-discharge for Sa120-d. This result confirms the occurrence of an acid attack of the clay particles in the post-discharge. Indeed, the specific surface area of clay generally increases during acid treatment as reported in [36, 37].

Table 2 Assignment of new hydroxyl bands formed after plasma treatment of clay

Bands (cm^{-1})	Functional groups	Illustration
3,750	Isolated silanols or geminal silanols	Si-OH OH Si OH
3,730	Vicinal silanols weakly bonded	H O H O Si Si
3,668	Internal silanols	–
3,649	Vicinal silanols strongly bounded	H O H O H O Si Si Si

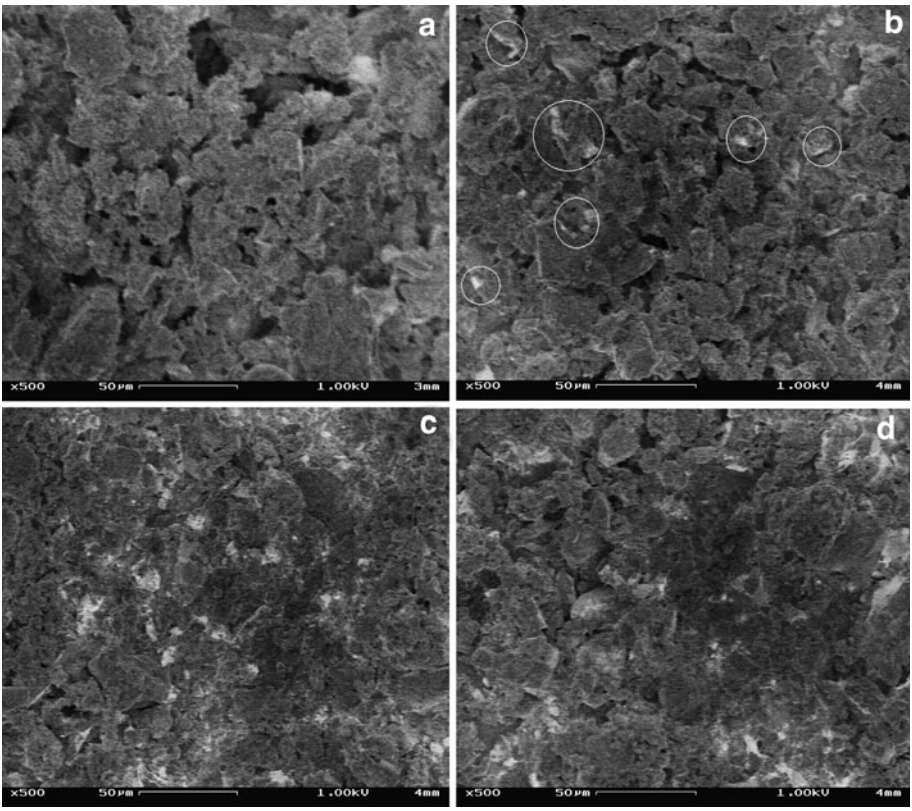

Fig. 11 SEM micrographs of untreated (**a** Sa00-00) and plasma treated clays (**b** Sa120-00, **c** Sa30-48, **d** Sa120-48)

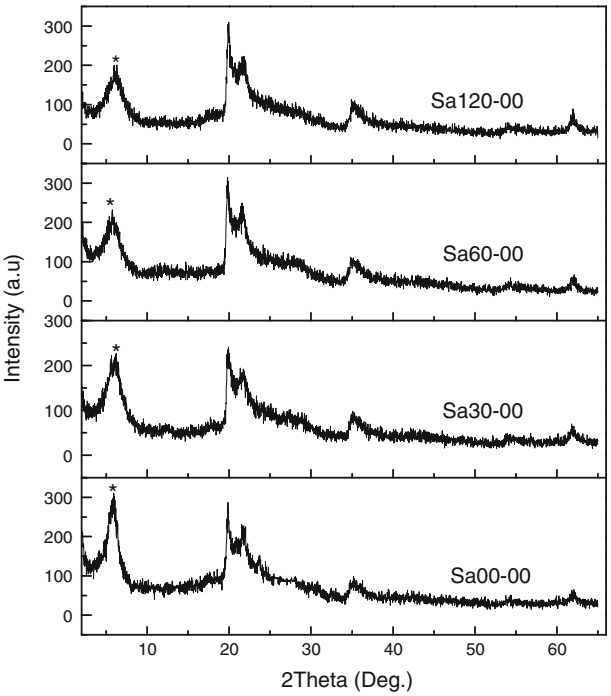

Fig. 12 XRD patterns of clay samples before and after plasma treatment (*asterisk*: d_{001} band of smectite)

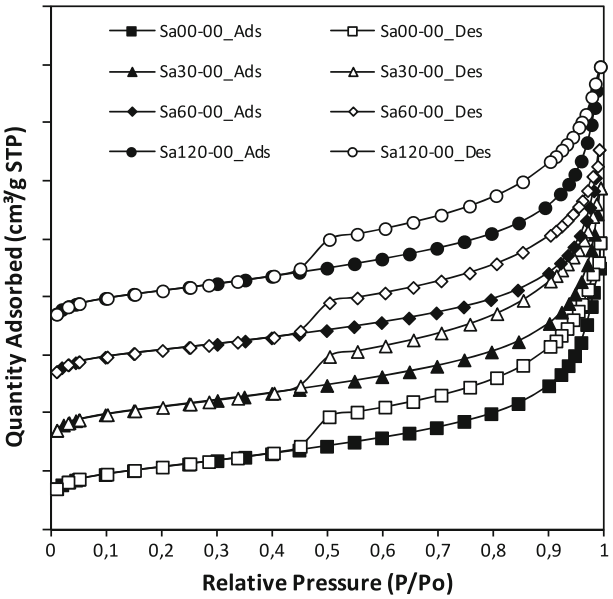

Fig. 13 Adsorption-desorption isotherms of nitrogen on untreated and plasma treated clays

Table 3 Surface area and pore volume of untreated and plasma treated clays

	BET surface area			Pore volume	
	S_{BET} ($m^2\ g^{-1}$)	$S_{micropores}$ ($m^2\ g^{-1}$)	$S_{ext.}$ ($m^2\ g^{-1}$)	V_{Total} ($mL\ g^{-1}$)	$V_{micropores}$ ($mL\ g^{-1}$)
Sa00-00	38	7.2	30.9	0.069	0.003
Sa30-00	39	6.6	32.8	0.069	0.003
Sa30-06	39	8.2	31.2	0.071	0.004
Sa30-12	35	8.0	26.4	0.064	0.004
Sa30-24	39	6.5	33.1	0.070	0.003
Sa30-48	37	6.3	30.9	0.068	0.003
Sa120-00	39	8.4	30.3	0.065	0.004
Sa120-06	39	7.8	31.1	0.063	0.003
Sa120-12	42	7.9	34.1	0.074	0.003
Sa120-24	42	6.8	34.8	0.072	0.003
Sa120-48	45	10.3	34.3	0.074	0.004

Conclusion

Smectite clay from Sabga (Cameroon) was treated in aqueous suspension by gliding arc plasma at atmospheric pressure. The results of FTIR analysis suggest that plasma treatment induces the formation of silanol and new aluminol groups on the clay surface due to the reactive radicals ($HO^{\cdot}$ and $NO^{\cdot}$) present in humid air plasma medium. Only few slight crystalline and textural modifications of clay minerals are observed as due to the plasma. Exposure of the clay suspension on plasma discharge for long time (120 min) induces an acidification of the medium that induces afterward in the post-discharge treatment a partial degradation of clay particles through acid attack. This feature presents a noticeable interest for environmental applications. Indeed moderate plasma treatments are shown here to bring about a beneficial activation of adsorption sites (silanols and aluminols), still preserving intact the more macroscopic features (texture end structure) of the clay.

Acknowledgments The authors thank the "Université catholique de Louvain" (Belgium) for the grant awarded to A.T.D. in the frame of the fellowship "Coopération au développement" program.

References

1. Ciullo P-A (1996) Industrial Minerals and their uses: a handbook and formulary. William Andrew Inc., New Jersey
2. Njopwouo D, Roques G, Wandji R (1988) A contribution to the study of the catalytic action of clays on the polymerisation of styrene: II. Reaction mechanism. Clay Miner 23:35–43
3. Murray H (2000) Traditional and new applications for kaolin, smectite, and palygorskite: a general overview. Appl Clay Sci 17:207–2214
4. Torres Sanchez R-M, Genet M-J, Gaigneaux E-M, Dos Santos Afonso M, Yunes S (2011) Benzimidazole adsorption on the external and interlayer surfaces of raw and treated montmorillonite. Appl Clay Sci 53:366–373
5. Onal M (2007) Changes in crystal structure, thermal behavior and surface area of bentonite by acid activation. Commun Fac Sci Univ Ank B 53:1–14
6. Bergaya F, Aouad A, Mandalia T (2006) Pillared clays and clay minerals. Handb Clay Sci 1:393–421

7. Tonle I-K, Ngameni E, Njopwouo D, Carteret C, Walcarius A (2003) Functionalization of natural smectite-type clays by grafting with organosilanes: physico chemical characterization and application to mercury (II) uptake. Phys Chem Chem Phys 5:4951–4961
8. Benstaali B, Cheron B, Addou A, Brisset J-L (1999) Spectral investigation of a gliding arc in humid air: a key for chemical applications. In: Proceedings of the IUPAC Congress ISPC-14 (Int. Symp. Plasma Chem.; Praga, Czech Rep. 2), pp 939–944
9. Czernichowski A, Nassar H, Ranaivoloarimanana A, Fridman A, Simek M, Musiol K, Pawelec E, Dittrichova L (1996) Spectral and electrical diagnostics of the gliding arc. Acta Phys Pol, A 89:595–603
10. Hnatiuc E (2002) Electrical methods of measurement and treatment of pollutants. Tech & Doc, Lavoisier, Paris
11. Benstaali B, Boubert P, Cheron B, Addou A, Brisset J-L (2002) Density and rotational temperature measurements of the NO and OH radicals produced by a gliding arc in humid air and their interaction with aqueous solutions. Plasma Chem Plasma Process 22:553–571
12. Delair L, Brisset J-L, Cheron B (2001) Spectral, electrical and dynamic analysis of a 50 Hz air gliding arc. J High Temp Mater Process 5:381–402
13. Fanmoe J, Kamgang J-O, Moussa D, Brisset J-L (2003) Application de l'arc glissant d'air humide au traitement des solvants industriels: cas du 1,1,1-trichloroethane. Phys Chem News 14:1–4
14. Tchoumkwe C–C, Kuete Saa D, Laminsi S, Njopwouo D, Hnatiuc E (2012) Plasmachemical decolouration of 2, 4-dinitrophenylhydrazine by gliding electric discharge at atmospheric pressure. Int J Curr Res 4:70–75
15. Njoyim-Tamunganga E, Laminsi S, Ghogomu P, Njopwouo D, Brisset J-L (2011) Pollution control of surface waters by coupling gliding discharge treatment with incorporated oyster shell powder. Chem Eng J 173:303–308
16. Katsumura Y (1998) NO_2 and NO_3 radicals in radiolysis of nitric acid solutions. In: Alfassi Z (ed) N centered radicals, Chap 12. Wiley, Chichester, pp 393–412
17. Doubla A, Bouba L, Fotso M, Brisset J-L (2007) Plasmachemical decolourization of bromothymol blue by gliding arc discharge. Dyes Pigm 77:118–124
18. Pascal S, Moussa D, Hnatiuc E, Brisset J-L (2010) Plasma chemical degradation of phosphorous-containing warfare agents stimulants. J Hazard Mater 175:1037–1041
19. Moussa D, Brisset J-L (2003) Disposal of spent tributylphosphate by gliding arc plasma. J Hazard Mater 102:189–200
20. Eren E (2009) Removal of basic dye by modified Unye bentonite. J Hazard Mater 162:1355–1363
21. He H, Ma Y, Zhu J, Yuang P, Qing Y (2010) Organoclays prepared from montmorillonitees with different cation exchange capacity and surfactant configuration. Appl Clay Sci 48:67–72
22. Djoufac Woumfo E, Kamga R, Figueras F, Njopwouo D (2007) Acid activation and bleaching capacity of some Cameroonian smectite soil clays. Appl Clay Sci 37:149–156
23. Lesueur H, Czernichowsky A, Chapelle J (1988) A device for the formation of low temperature plasma by means of gliding electric discharges. Fr Pat 2639172
24. Czernichowski A (2001) Glidarc assisted preparation of the synthesis gas from natural and waste hydrocarbons gases. Oil & gas science and technology—Rev. IFP 6:181–198
25. Madejóva J, Bujdak J, Janek M, Komadel P (1998) Comparative FT-IR study of structural modifications during acid treatment of dioctahedral smectites and hectorite. Spectrochimica Acta Part A 54:1397–1406
26. Madejóva J, Komadel P (2001) Baseline studies of the clay minerals society source clays: infrared methods. Clays Clay Miner 49:410–432
27. Ming H, Spark K-M (2003) Radio frequency plasma-induced hydrogen bonding on kaolinite. J Phys Chem 107:694–702
28. Laminsi S, Acayanka E, Ndifon P-T, Nzali S, Brisset J-L (2012) Direct impact and delayed post-discharge chemical reactions of Fe^{II} complexes induced by non-thermal plasma. Deswater 37:38–45
29. Laminsi S, Acayanka E, Ndifon P-T, Tiya A-D, Brisset J-L (2012) Plasmachemical dissociation and degradation of naphtol green B complex. Env Eng Manag J 11:1461–1466
30. Dugas V, Chevalier Y (2003) Surface hydroxylation and silane grafting on fumed and thermal silica. J Colloid Interface Sci 264:354–361
31. Khraisheh M-A-M, Al-Ghouti M-A, Allen S-J, Ahmad M-N (2005) Effect of OH and silanol groups in the removal of dyes from aqueous solution using diatomite. Water Res 39:922–932
32. Chang Ming D, Dong Wei H, Hong Xia L, Mu Dan Xiao, Kui W, Lu Z, Zhi Yi Li, Teng Fei C, Jian Min M, Dong G, Yu Hao H, Shang Kun L, Liao Y, Chuang Rong Z (2013) Adsorption of acid orange II from aqueous solution by plasma modified activated carbon fibers. Plasma chem. Plasma process 33:65–82
33. Douglas L-A, Fiessinger F (1971) Degradation of clay minerals by H_2O_2 treatments to oxidize organic matter. Clays Clay Miner 19:67–68

34. Sing K-S-W, Everett D-H, Haul R-A-W, Moscou L, Pierotti R-A, Rouquérol J, Siemieniewska T (1985) Reporting physisorption data for gas/solid systems with special reference to the determination of surface area and porosity. Pure Appl Chem 57:603–619
35. Adkins B-D, Davis B-H (1988) Comparison of nitrogen adsorption and mercury penetration results I. Pore volume and surface area obtained for type IV isotherms. Adsorpt Sci Technol 5:76–93
36. Nguetnkam J-P, Kamga R, Villiéras F, Ekodeck G-E, Razafitianamaharavo A, Yvon J (2005) Assessment of surface areas of silica and clay in acid-leached clay materials using concepts of adsorption on heterogeneous surfaces. J Colloid Interface Sci 289:104–115
37. Temuujin J, Jadambaa T-S, Burmaa G, Erdenechimeg S, Amarsanaa J, MacKenzie K-J-D (2004) Characterisation of acid activated montmorillonite clay from Tuulant (Mongolia). Ceram Int 30:251–255